MASTER COPY . KEEP THIS COPY FOR REPRODUCTION PURPOSES

REPORT DOCUMENTATION PAGE

Form Approved
OMB No. 0704-0188

1. AGENCY USE ONLY (Leave blank)	2. REPORT DATE	3. REPORT TYPE AND DATES COVERED
	8/11/95	Final Report

4. TITLE AND SUBTITLE
Electroluminescing Porous Silicon ELPS Device

5. FUNDING NUMBERS
DAAH04-93-G-0240

6. AUTHOR(S)
John Penczek and Rosemary L. Smith

7. PERFORMING ORGANIZATION NAME(S) AND ADDRESS(ES)
Dept of Electrical and Computer Engineering
University of California, Davis
Davis, CA 95616

8. PERFORMING ORGANIZATION REPORT NUMBER

9. SPONSORING/MONITORING AGENCY NAME(S) AND ADDRESS(ES)
U.S. Army Research Office
P.O. Box 12211
Research Triangle Park, NC 27709-2211

10. SPONSORING/MONITORING AGENCY REPORT NUMBER
ARO 31556.3-EL

11. SUPPLEMENTARY NOTES
The views, opinions and/or findings contained in this report are those of the author(s) and should not be construed as an official Department of the Army position, policy, or decision, unless so designated by other documentation.

12a. DISTRIBUTION/AVAILABILITY STATEMENT
Approved for public release; distribution unlimited.

12b. DISTRIBUTION CODE

13. ABSTRACT *(Maximum 200 words)*

The main goal of this project was to determine the mechanism of operation of an all silicon, electroluminescing device. The device consists of an n+ silicon "wire" supported on top of a layer of porous silicon. Other aims included the evaluation of the device's light emitting efficiency and it's potential as a silicon-based light source. The device emits light over a broad spectrum, extending from the visible into the infrared, with two dominant peaks, at 1.3 and 2.05 microns. An optical quantum efficiency of better than 6% was determined. The device demonstrated continuous device operation for over 150 hours. The spectral data strongly suggests that blackbody radiation is the dominant emission mechanism in our device. However, there is also evidence of hot electron induced emission. We suspect that hot electrons are injected into the interface with the underlying porous silicon, from which some of the emission originates.

14. SUBJECT TERMS	15. NUMBER OF PAGES
Porous Silicon, Light-emitting Silicon Electroluminescing Porous Silicon	13
	16. PRICE CODE

17. SECURITY CLASSIFICATION OF REPORT	18. SECURITY CLASSIFICATION OF THIS PAGE	19. SECURITY CLASSIFICATION OF ABSTRACT	20. LIMITATION OF ABSTRACT
UNCLASSIFIED	UNCLASSIFIED	UNCLASSIFIED	UL

ELECTROLUMINESCING POROUS SILICON (ELPS) DEVICE

Final Report
June 1993-June 1995

John Penczek and Rosemary L. Smith

August 11, 1995

U.S. ARMY RESEARCH OFFICE

DAAH04-93-G-0240

Dept. of Electrical and Computer Engineering
UNIVERSITY OF CALIFORNIA, DAVIS

APPROVED FOR PUBLIC RELEASE;
DISTRIBUTION UNLIMITED

FORWARD

The dominance of silicon as an electronic material has long motivated researchers to find a silicon emitter for integrated optoelectronics. An efficient silicon light emitter would make a significant impact in communications, optical interconnects, and display technologies. The main impediment in realizing a silicon light source has been the indirect band structure of crystalline silicon, which makes radiative transitions improbable. In spite of this fact, early work on avalanche breakdown in reverse biased silicon p-n junctions[1,2] demonstrated that current-induced visible emission was possible. The emission was found to be quite broad, with a peak in the near-infrared[3]. However, their low quantum efficiencies made them impractical for optoelectronic applications. Similar weak visible emission was also observed in small geometry silicon metal-oxide-semiconductor field-effect transistors (MOSFETs)[4,5]. This visible emission was attributed to hot carrier injection produced by the high fields at the drain boundary.

More recently, the report of efficient room temperature photoluminescence (PL) from porous silicon[6] has created new hope for silicon optoelectronics. The physical mechanism responsible for porous silicon PL is still not well understood. The main models proposed for porous silicon PL involve: a chemical agent on the surface, surface or interface states, and a quantum confinement effect. A recent proposal suggests that the experimental data is best explained by the combination of quantum confinement and surface states[7]. Since the announcement of visible PL, a variety of porous silicon Schottky barrier and p-n junction structures have demonstrated visible electroluminescence (EL)[8-12]. Most of these structures had rectifying electrical characteristics. The EL emission was usually similar to the PL spectra, with a full-width-at-half-maximum of about 120 nm. One report of a porous silicon EL device demonstrated that even blue light emission[13] was possible. In addition to visible emission, near-infrared PL and EL have also been observed from porous silicon samples[14-17]. Sreseli[17] demonstrated broad near-infrared EL emission from porous silicon using a liquid contact.

In September, 1992, we fabricated an all silicon device, which when electrically biased emitted a bright orange light, clearly visible under normal room lighting. This device included a layer of porous silicon. It's electrical characteristics were unusual: a negative differential resistance commenced at the onset of visible luminescence and the device was very stable, operating continuously without any substantial decay for several days, despite high excitation power (100 mW). This project was initiated to determine the mechanism of device operation.

TABLE OF CONTENTS

LIST OF FIGURES

PROBLEM STATEMENT:

The objectives of the project did not deviate from those originally stated in the proposal. The main goal was to determine the mechanism of operation of an electroluminescing porous silicon device which was fabricated in our facility. Other aims include evaluation of device efficiency and potential as a silicon-based light source.

SUMMARY OF IMPORTANT RESULTS

- Created a monolithic broad band light source in silicon.
- Achieved better than 6% optical quantum efficiency.
- Demonstrated continuous device operation for over 150 hours.
- Developed a low temperature packaging process for porous silicon emitters.

DEVICE FABRICATION

The device developed under this research grant utilizes solid-state contacts to produce a broad spectrum emitter which peaks in the near-infrared. The porous silicon emitter was fabricated by diffusing phosphorous into a 9 Ω-cm p-type silicon wafer, creating 15 μm and 55 μm wide by 2.5 mm long n^+/p junctions. The phosphorous was diffused at 925 C, resulting in a 1.6 μm deep p-n junction. Aluminum was deposited on the back of the wafer and alloyed to establish an ohmic contact to the substrate. The silicon surface was then anodized in 20 wt% HF at 20 mA/cm^2, producing a 40 μm thick porous silicon layer (PSL). The selective etching of p-type silicon over n-type results in the formation of porous silicon around and under the phosphorous diffusion[18]. A schematic of the device structure is given in Figure 1.

Since the properties of porous silicon are known to change at elevated temperatures, and prolonged exposure to air and since its morphology and surface chemistry is very sensitive to any post-formation exposure to low or high pH solutions and organic solvents, we had a particularly difficult time developing a process for deposition and patterning a thin film metal contact to the devices. Many of the more standard, metallization processes used with crystalline silicon devices were found to be incompatible with porous silicon processing. A passivation layer of PECVD silicon nitride was initially attempted, since it involves relatively low temperatures (≤ 350C) and nitride is an excellent oxygen and moisture barrier. However, the films were found to be too porous, and did not protect the porous silicon from chemical attack during the phololithography (hydroxide developer) and Al metal etching (nitrid acid) processes. Evaporated

and RF sputtered silicon dioxide passivation layers were then investigated. Of the two, the sputtered oxide was dense enough to provide a chemical barrier for the porous silicon during metal patterning. But standard wet etching procedures, with buffered HF acid, producing severe under-etching , presumedly due to the low density of the oxide. Therefore, a more anisotropic etch, such as reactive ion etching, needs to be used for patterning this passivation layer.

In addition to determining a suitable passivation and patterning process for porous silicon, the issues in developing a compatible interconnect technology for this material were also addressed. Early porous silicon device research identified that establishing electrical contact to porous silicon devices was problematic. Aluminum and gold wire bonding is often used in packaging silicon devices. However, neither of these techniques could be successfully applied to our devices since the contact regions lie directly over porous silicon, which is too fragile to withstand the ultrasonic scrubbing process. This difficulty requires that metallization lines be extended out past the porous silicon region so that wire bonding can be performed on bonding pads lying over crystalline silicon.

ELECTRICAL PROPERTIES

Electrical contact to the top n-type layer of the porous silicon emitter was usually made with a needle probe. Biasing between the n-layer and the substrate resulted in a rectifying junction, with forward bias defined by a negative potential applied to the n-layer relative to the substrate. Static current-voltage measurements were obtained with a Tektronix 370 curve tracer. Typical static current-voltage (I-V) curves of the 15 μm and 55 μm wide porous silicon emitters operating in forward bias are given in Figure 2. Both of these devices exhibited a region of current-controlled negative differential resistance (NDR), with the 15 μm wide device demonstrating a larger slope and current onset of NDR. The dynamic response was determined by modulating the current about a 14 mA DC offset and monitoring the optical signal versus modulation frequency. The optical emission was found to have a 3 dB rolloff at 550 Hz.

The observed NDR may be attributeable to thermal effects. The surface temperature of an operating emitter was measured by a fine-tip thermocouple to be about 250 C. The reverse bias leakage current of crystalline silicon p-n juctions start to leak considerable at this temperature due to the thermal generation of carriers inside the space charge region. Thermally generated carriers within the porous silicon layer could produce a significant reduction in resistance, since at room temperature, it is close to intrinsic. The I-V characteristics near and above the onset of NDR change slowly over time, with the onset point moving to higher current and voltage values. However, a lifetime study (described below) demonstrates that the devices can be operated continuously for more than a week.

OPTICAL PROPERTIES

The onset of visible emission can be observed along the n-layer with dark-adapted eyes at about 9 mA for the 55 μm device. The bright red-orange emission can be easily seen under normal room lighting at drive currents above 15 mA. Using a CCD camera, the emission intensity was found to be uniform along the length of the n-layer, with a broad maximum in the middle of its 55 μm width. Spectral measurements were taken at room temperature with a *f*/4 24 cm monochromator (CVI Digikrom 240) using an S1 photomultiplier tube (PMT) and a liquid nitrogen cooled InSb detector. The visible and infrared spectra were combined by making the appropriate normalization where the two spectra overlapped. The current-induced emission measurements were taken with the device operating under constant current conditions, and under low duty cycle (10% at 10 Hz) pulsed current conditions. All spectra were corrected for the instrument system response. The PL and current-induced spectra taken from the porous silicon emitter are shown in Figure 3. The PL spectrum is centered at 794 nm with a full-width-at-half-maximum of 136 nm. Near-infrared PL could not be resolved from our sample, although PL near 1.3 μm is often observed[14-16] from porous silicon samples. The current-induced spectrum is relatively broad, with a silicon sub-bandgap peak near 1.3 μm. Spectra measured under constant current and pulsed current operation yielded the same spectral characteristics. The spectral features in the near-infrared do not shift in wavelength as the drive current is varied, however, the 1.3 μm peak intensity grows relative to the 2.1 μm emission band with increasing current. The visible component of the EL spectrum has a long high energy tail which extends into the blue. Even blue emission at 420 nm can be observed with the naked eye using a bandpass filter. The emission spectra from the 15 μm device gave similar results.

The quantum efficiency of the current-induced emission was determined by initially measuring the spatially integrated power at one wavelength using an integrating sphere. Once the total power emitted at that wavelength was known, the rest of the emission spectra could be scaled to absolute power units. A spectral integration yielded a quantum efficiency of better than 6% at 25 mA for the 55 μm device. The total power emitted is greater than 1 mW with a wall-plug efficiency of about 0.04%. These values are to be viewed as lower bounds, since the device emits beyond our measurement range.

LONG-TERM DEVICE BEHAVIOR

A investigation on the long-term stability of our device was conducted by monitoring the current-induced emission at 1.3 μm over a prolonged period. The device was operated at constant current, in air, and at room temperature. Figure 4 demonstrates continuous operation of a 55 μm wide junction for more that 150 hours. The 10 mA data seems to settle after an initial decrease in intensity, while the 20 mA data shows a gradual increase in intensity over time. A

subsequent pulsed experiment, in which the emission is excited by 10 Hz constant current pulses at 10% duty cycle, showed even greater stability over similar time periods. This indicates that the device instability has a thermal component, which may be alleviated by operating the device in pulsed mode.

EMISSION MECHANISM

The significant difference between the PL and current-induced spectra indicate at least two distinct emission mechanisms operating in our device. In addition, devices fabricated with different formation conditions and crystal orientation produced similar current-induced spectra. This insensitivity to porous silicon morphology suggested that the emission does not originate from the porous silicon. Given the high operating voltages of our device, the most likely candidates that may be responsible for the broad emission produced from our device are hot electron emission and blackbody radiation. When the current-induced emission measured by the monochromator (from Figure 3) is converted to photon emission per unit energy, a semi-log plot (Figure 5) demonstrates that the visible emission has an exponential dependence on photon energy. This spectral behavior is characteristic of the hot carrier emission observed from MOSFETs[4,5] and the avalanche breakdown spectra from p-n junctions[2]. A near-infrared emission peak is also commonly observed in the MOSFET[5] and p-n junction[3] spectra. However, the reported values of quantum efficiency from reverse biased silicon p-n junctions is typically on the order of 0.001%[19]. This is several orders of magnitude worse than that measured for our porous silicon device. A direct comparison of emitted optical power demonstrated that our forward biased porous silicon emitter produced far more intense emission than its crystalline silicon counterpart operated in the avalanche breakdown regime Under the same measurement conditions, the optical power emitted at 710 nm from the p-PSL-n structure was more than $5x10^4$ times greater than the crystalline p-n junction.

A blackbody contribution to the observed spectra was initially discounted since the 1.3 μm peak required a blackbody temperature that was 400 C above the melting point of silicon. However, a recent spectrum taken with a blackbody source fabricated from a suspended crystalline silicon filament also exhibited a peak near 1.3 μm. This peak may be the result of a sudden change in emissivity produced by an absorption change for photon energies near the bandgap[20]. When the filament emission $W(\lambda)$ is plotted as $\ln(\lambda^5 W(\lambda))$ versus $1/\lambda$ (Figure 6), a blackbody temperature of 1200 C can be extracted from the slope in the high absorption part of the spectrum. A similar procedure used on the porous silicon data from Figure 3 gives two slopes with blackbody temperatures of 1,140 C and 12,600 C. The lower temperature corresponds to a blackbody emission peak at 2.05 μm. The spectrum given in Figure 3 shows

only a weak peak at that wavelength. But its relative intensity may be weaker in comparison to the 1.3 μm peak due to the low emissivity in this low absorption region of the spectrum. The higher temperature is too large to be explained by blackbody radiation, but may be a result of hot electron emission.

In summary, we have fabricated a porous silicon device with broad current-induced emission. The current data strongly suggests that blackbody radiation is the dominant emission mechanism in our device. However, a contribution from hot electron emission can not be ruled out. Especially in light of the fact that some reverse-biased silicon diode spectra can closely match a blackbody spectrum[21].

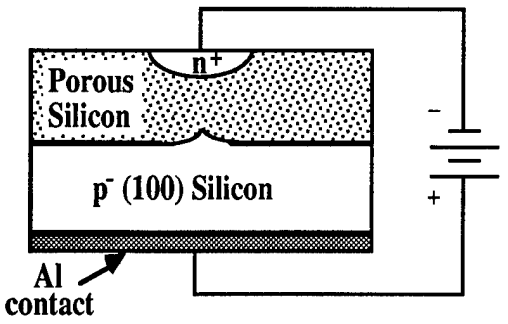

Figure 1: Porous silicon emitter structure in forward bias configuration.

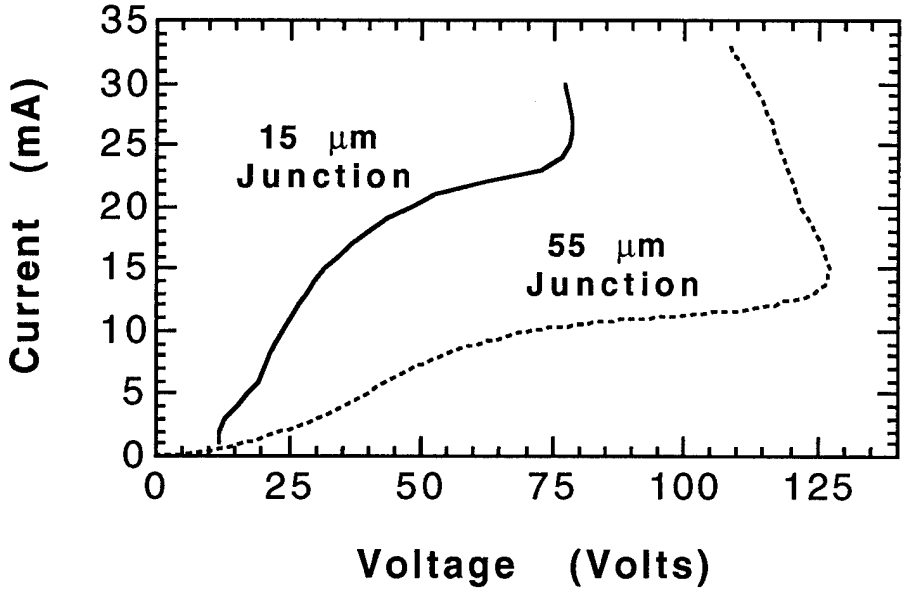

Figure 2: Static I-V behavior of 15 μm and 55 μm wide junctions under forward bias.

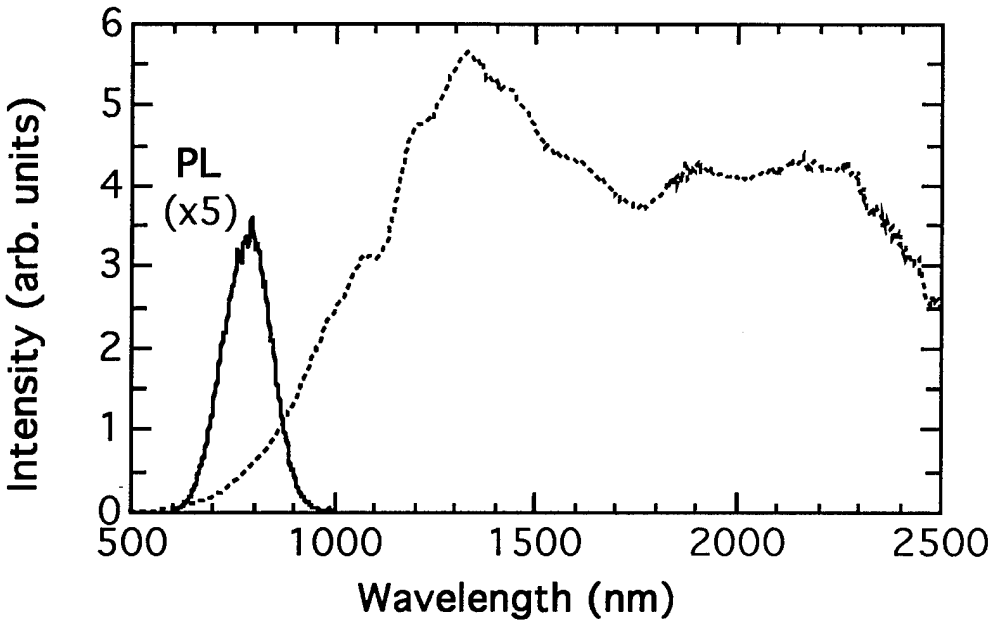

Figure 3: PL (solid) and current-induced (dashed) spectra from a porous silicon emitter. PL was measured under 50 mW/cm^2 of CW excitation at 527 nm. The current-induced spectrum was taken from a 55 μm wide junction forward biased at 30 mA.

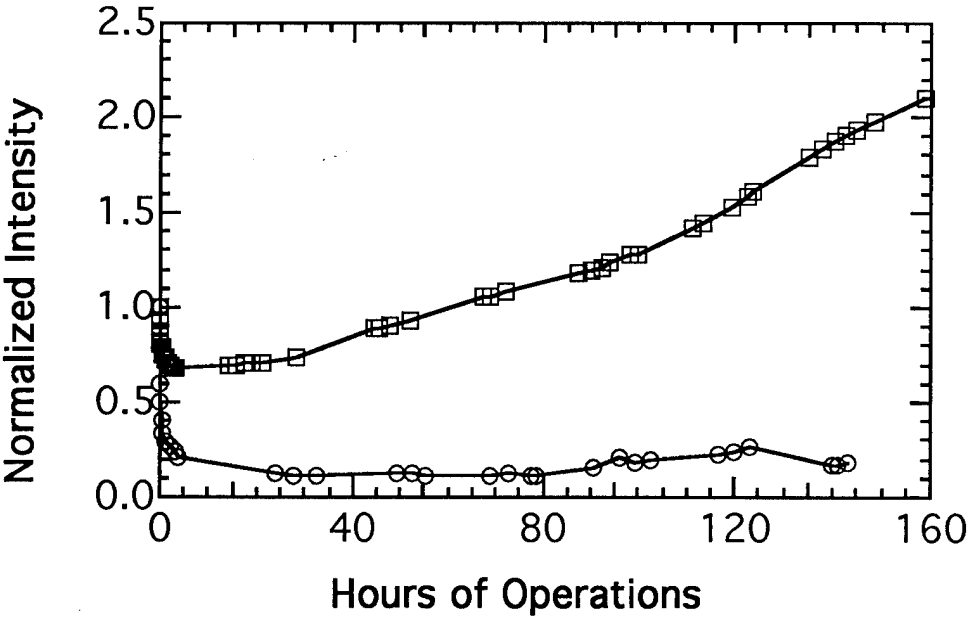

Figure 4: Time dependence of emission at λ=1.3 μm for 55 μm wide junction structure. Device was continuously operated at 10 mA (circles) and 20 mA (squares) constant current under ambient conditions.

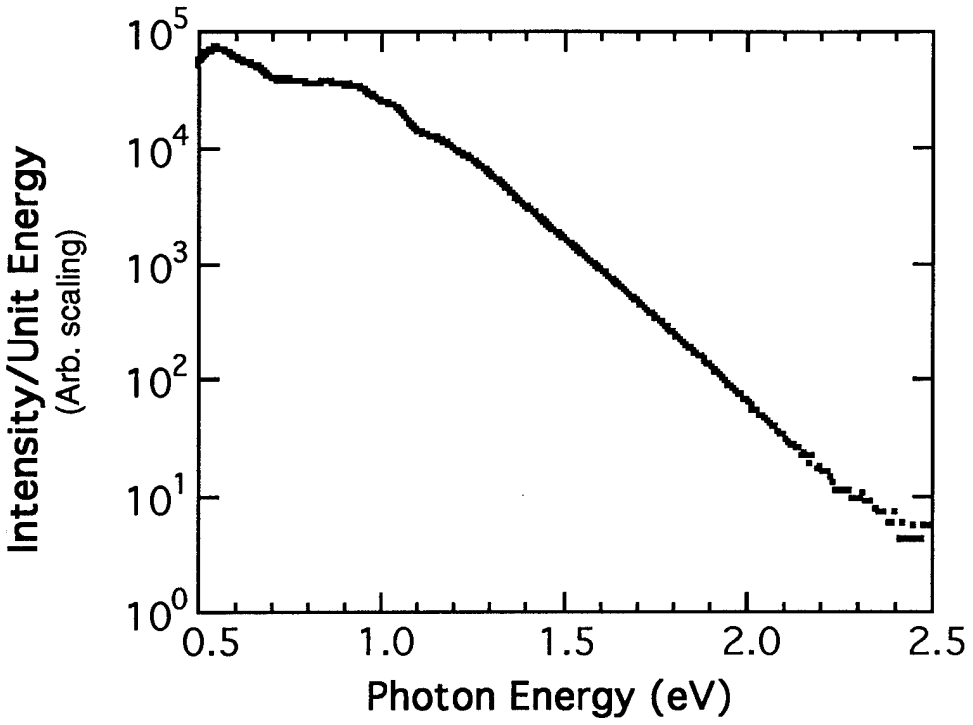

Figure 5: Semi-log plot of photon emission per unit energy from a forward biased porous silicon emitter demonstrates the exponential dependence of the visible emission. The data was converted from the current-induced spectrum in Figure 3.

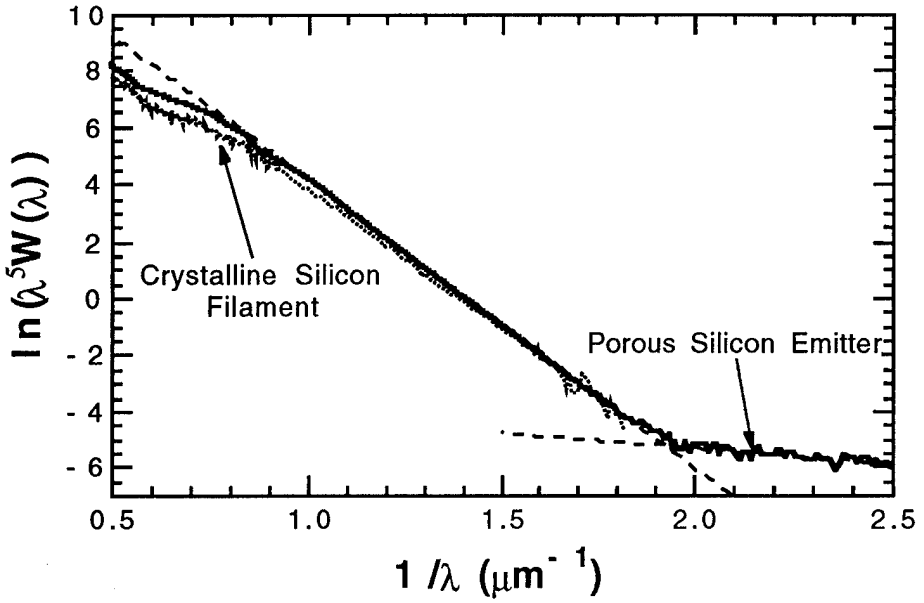

Figure 6: Comparison of silicon blackbody filament (solid line) with porous silicon emitter (dotted line). For an ideal blackbody, the temperature of the blackbody can be extracted from the slope (dashed lines).

PUBLICATIONS

1993 J. Penczek and R. L. Smith.
THE RELATIONSHIP OF POROUS SILICON FILM MORPHOLOGY TO THE PHOTO-LUMINESCENCE SPECTRA.
Proceedings of the Spring Meeting of Materials Research Society, Vol. 298.

1994 J. Penczek, I-W. Chao, A. Knoesen, H. Lee, J. E. Davis, and R. L. Smith.
VISIBLE TO NEAR-INFRARED EMISSION FROM A POROUS SILCON DEVICE.
IEEE LEOS Annual Meeting, Boston, MA.

1995 J. Penczek, I-Wen Chao, A. Knoesen, J. E. Davis, H. W. H. Lee, and R. L. Smith.
VISIBLE TO NEAR-INFRARED POROUS SILICON LIGHT EMITTING DEVICE.
Submitted to Applied Physics Letters.

PARTICIPATING SCIENTIFIC PERSONNEL

Technical Assistants:

Raffi Garabedian

Kirti Patel

Juliana Tu

Graduate Research Assistants:

John Penczek (PhD candidate: expected completion, Dec. 1995)

Post-Doctoral Associate:

David Barnes

Principal Investigators:

Prof. Scott D. Collins

Prof. Andre Knoesen

Prof. Rosemary L. Smith

BIBLIOGRAPHY

[1]R. Newman, Phys. Rev. **100**, 700 (1955)

[2]A. G. Chynoweth and K. G. McKay, Phys. Rev. **102**, 369 (1956)

[3]W. Haecker, Physica Status Solidi **25**, 301 (1974)

[4]A. Toriumi, M. Yoshimi, M. Iwase, Y. Akiyama, and K. Taniguchi, IEEE Trans. Electron Dev. **ED-34**, 1501 (1987)

[5]N. C. Das and B. M. Arora, Appl. Phys. Lett. **56**, 1152 (1990)

[6]L. T. Canham, Appl. Phys. Lett. **57**, 1046 (1990)

[7]F. Koch, V. Petrova-Koch, and T. Muschik, J. Luminescence **57**, 271 (1993)

[8]A. Richter, P. Steiner, F. Kozlowski, and W. Lang, IEEE Electron Dev. Lett. **12**, 691 (1991)

[9]N. Koshida and H. Koyama, Appl. Phys. Lett. **60**, 347 (1992)

[10]F. Namavar, H. P. Maruska, and N. M. Kalkhoran, Appl. Phys. Lett. **60**, 2514 (1992)

[11]E. Bassous, M. Freeman, J. M. Halbout, S. S. Iyer, V. P. Kesan, P. Mungia, S. F. Pesarcik, and B. L. Williams, Mater. Res. Soc. Symp. Proc. **256**, 23 (1992)

[12]Z. Chen, G. Bosman, and R. Ochoa, Appl. Phys. Lett. **62**, 708 (1993)

[13]P. Steiner, F. Kozlowski, and W. Lang, IEEE Electron Dev. Lett. **14**, 317 (1993)

[14]F. Koch and A. Kux, Mater. Res. Soc. Symp. Proc. **298**, 391 (1993)

[15]S. Gardelis, P. Dawson, and B. Hamilton, Mater. Res. Soc. Symp. Proc. **298**, 337 (1993)

[16]P. M. Fauchet, E. Ettedgui, A. Raisanen, L.J. Brillson, F. Seiferth, S. K. Kurinec, Y. Gao, C. Peng, and L. Tsybeskov, Mater. Res. Soc. Symp. Proc. **298**, 271 (1993)

[17]O. Sreseli, V. Petrova-Koch, D. Kovalev, T. Muschik, S. Hofreiter, and F. Koch, in *Proceedings of the 22nd Int. Conf. Physics of Semiconductors, Vancouver, 1994*

[18]K. Imai and H. Unno, IEEE Trans. Electron Devices **ED-31**, 297 (1984)

[19]L. A. Kosyachenko, E. F. Kukhto, and V. M. Sklyarchuk, Soviet Phys. Semiconductors **18**, 266 (1984)

[20]P. J. Timans, J. Applied Phys., **74**, 6353 (1993)

[21]L. A. Kosyachenko, E. F. Kukhto, V. M. Sklyarchuk, and V. A. Shemyakin, Soviet J. Optical Technol. **57**, 385 (1990)